Molecular Medicine

Renal Integrin-Linked Kinase Depletion Induces Kidney cGMP-Axis Upregulation: Consequences on Basal and Acutely Damaged Renal Function

José Luis Cano-Peñalver,[1,2] Mercedes Griera,[1,2] Andrea García-Jerez,[1,2] Marco Hatem-Vaquero,[1,2] María Piedad Ruiz-Torres,[1,2] Diego Rodríguez-Puyol,[2,3] Sergio de Frutos,[1,2] and Manuel Rodríguez-Puyol[1,2*]*

[1]Department of Systems Biology, Physiology Unit, Universidad de Alcalá, Alcalá de Henares, Madrid, Spain; [2]Instituto Reina Sofia de Investigación Renal and REDinREN from Instituto de Salud Carlos III, Madrid, Spain; [3]Biomedical Research Foundation and Nephrology Department, Hospital Príncipe de Asturias, Alcalá de Henares, Madrid, Spain

Soluble guanylyl cyclase (sGC) is activated by nitric oxide (NO) and produces cGMP, which activates cGMP-dependent protein kinases (PKG) and is hydrolyzed by specific phosphodiesterases (PDE). The vasodilatory and cytoprotective capacity of cGMP-axis activation results in a therapeutic strategy for several pathologies. Integrin-linked kinase (ILK), a major scaffold protein between the extracellular matrix and intracellular signaling pathways, may modulate the expression and functionality of the cGMP-axis–related proteins. We introduce ILK as a novel modulator in renal homeostasis as well as a potential target for cisplatin (CIS)-induced acute kidney injury (AKI) improvement. We used an adult mice model of depletion of ILK (cKD-ILK), which showed basal increase of sGC and PKG expressions and activities in renal cortex when compared with wildtype (WT) littermates. Twenty-four h activation of sGC activation with NO enhanced the filtration rate in cKD-ILK. During AKI, cKD-ILK maintained the cGMP-axis upregulation with consequent filtration rates enhancement and ameliorated CIS-dependent tubular epithelial-to-mesenchymal transition and inflammation and markers. To emphasize the role of cGMP-axis upregulation due to ILK depletion, we modulated the cGMP axis under AKI *in vivo* and in renal cultured cells. A suboptimal dose of the PDE inhibitor ZAP enhanced the beneficial effects of the ILK depletion in AKI mice. On the other hand, CIS increased contractility-related events in cultured glomerular mesangial cells and necrosis rates in cultured tubular cells; ILK depletion protected the cells while sGC blockade with ODQ fully recovered the damage.

Online address: http://www.molmed.org
doi: 10.2119/molmed.2015.00059

INTRODUCTION

Despite breakthroughs in basic research and medical care, the therapeutic approaches to acute kidney injury (AKI) are unsatisfactory. The pathogenesis of AKI involves changes in the oxygenation of renal structures as a consequence of vascular dysfunction and direct cellular damage induced by exogenous toxins, lipoproteins or local mediators. Nephrotoxicity occurs at both the glomerular and tubular levels (1–3) and involves multiple mechanisms, including tubular apoptosis and cell death, inflammation, oxidative stress and hypoxia. During AKI, there is an increase of proinflammatory cytokines such as monocyte chemoattractant protein-1 (MCP-1) and transforming growth factor β (TGF-β), which promotes the progression of tubular epithelial-to-mesenchymal transition (EMT) (1–3). EMT is a condition characterized by an increase in mesenchymal markers such as α–smooth muscle actin (α-SMA) (4,5). The final consequence of AKI is impaired glomerular and tubular function (6–8).

Cyclic GMP (cGMP) is an intracellular messenger that regulates vascular smooth muscle cell and glomerular mesangial cell contraction, thus its upregulation leads to vascular dilation (9). Furthermore, there is abundant literature pointing to the relevant cytoprotective effect of agents that increase cGMP, which have been shown to be beneficial under several clinical and experimental conditions (10–12) including renal protection under nephrotoxic agents (13–16). However, the nature of this protection has not been definitively elucidated. Elucidation, which could help, determine the prevention or even the treatment of AKI.

**SdF and MR-P have contributed equally to the direction of this work.*

Address correspondence to *Sergio de Frutos, Departamento de Biología de Sistemas, Unidad Fisiología, Facultad de Medicina, Universidad de Alcalá, 28805 Alcalá de Henares, Madrid, Spain. Phone: +34-91-8854519; Fax: +34-91-8854590; E-mail: sergio.frutos@uah.es.*
Submitted March 18, 2015; Accepted for publication November 9, 2015; Published Online (www.molmed.org) November 10, 2015.

The NO binding to the soluble guanylyl cyclase (sGC) heterodimer, of which the α1 and β1 subunit isoforms predominate in the kidney (17) and are required for sGC activity (18), starts the cGMP production which interacts with downstream effectors such as cGMP-gated channels, the cGMP-dependent protein kinase type I family (PKG Iα and Iβ) (19) and the phosphodiesterases (PDE) (specifically PDE5) hydrolyzing the cGMP (20). Considering the vasorelaxing and cytoprotective effects of cGMP, it could be suggested that NO donors currently available for human treatment are useful in AKI management. Unfortunately, clinical studies have failed to demonstrate this possible beneficial effect because sGC and PKG are quickly downregulated by NO (9,21). Our previous works have linked the sGC-cGMP-PKG system with the widely expressed intracellular scaffold protein integrin-linked kinase (ILK), which is part of the adhesome complex that modulates the outside extracellular matrix (ECM) signaling to the inside of the cell through the membrane-bound integrins (22–25). ECM modulates the cellular behavior through ILK by changing the cytoskeleton structure and gene transcription between other intracellular pathways. ILK is thus crucial in several processes and diseases, ranging from fibrosis to cancer (26). Our previous works, in conjunction with other authors, involved ILK or downstream effectors in inflammatory responses, EMT and fibrosis during renal damage (2,5,27–35). However the role of ILK during AKI remains elusive. Previously, we demonstrated ILK modulation of the cGMP system in primary cultured mesangial cells (23) and similar upregulation in the vascular smooth muscle from healthy adult mice with an ubiquitous conditional general inducible ILK depletion (cKD-ILK), which in turn responded better to cGMP-dependent vasodilators (25). In the present work, we explored *in vivo* and in cultured cells the ILK-based cGMP modulation of the glomerular filtration under either basal conditions or during cisplatin (CIS)-induced AKI.

MATERIALS AND METHODS

Ethical Approval

All procedures involving animals were previously approved by the University of Alcalá's Institutional Animal Care and Use Committee and conformed to Directive 2010/63/EU of the European Parliament. The animals were housed in a pathogen-free and temperature-controlled room (22°C ± 2°C). Food and water were available *ad libitum*.

Conditional ILK Knockdown Mice

The general inducible ILK knockdown mice (cKD-ILK) model has been explained extensively in prior publications (25,36). Briefly, conditional inactivation of the ILK gene was accomplished by crossing C57Bl/6 mice homozygous for the floxed ILK allele flanked by loxP sites with homozygous mice carrying a tamoxifen (TX)-inducible CreER(T) recombinase gene (CRE, CMV-Cre are from Jackson Laboratory with a strain of origin BALB/cJ). Two-month-old male CRE-LOX mice weighing 20 to 28 grams were injected intraperitoneally (IP) with 1.5 mg of TX (Sigma-Aldrich) or vehicle once a day for five consecutive days to induce ILK depletion. Three weeks after the injections, the tail DNA was genotyped by PCR. The TX-treated CRE-LOX mice displaying successful depletion of ILK were termed conditional knockdown-ILK (cKD-ILK) mice and the vehicle-treated CRE-LOX were termed wild-type (WT) mice.

In Vivo Experiments

Depending on the experimental approach selected, the mice were treated with one single dose of either NO donor isosorbide dinitrate (IDN) (300 mg/kg/day, gavage), vehicle (saline, IP), AKI inductor cisplatin (*cis*-diamminedichloroplatinum (II), CIS) (10 mg/kg IP) and/or PDE5 inhibitor Zaprinast (ZAP) (1,4-dihydro-5-(2-propoxyphenyl)-7H-1,2,3-triazolo[4,5-d] pyrimidine-7-one) (2.5 mg/kg, IP). All the treatments were from Sigma-Aldrich. The animals were housed in metabolic cages to collect 24 h urine. Basal blood samples were collected by inferior palpebral vein incision. After 24 h of IDN treatment or 72 h of vehicle, CIS and/or ZAP injections, the mice were euthanized and urine, blood and kidney samples were collected. Plasma and urine metabolites were determined with commercial kits according to the manufacturer's protocol: creatinine, blood urea nitrogen (BUN) (Arbor Assays LLC) and mouse urinary albumin (Abcam). From this point on, every spectophotometry determination was achieved with the Multimode Plate Reader Victor X4 (PerkinElmer).

Ex Vivo Experiments

Kidneys were freshly collected and the renal cortex was divided into slices and placed in culture dishes with DMEM-F12 medium (Lonza) at 37°C. In some experiments, the slices were pretreated with 100 μmol/L of the PDEs wide-range inhibitor 3-isobutyl-1-methylxanthine (IBMX, Sigma-Aldrich) for 15 min. The slices were incubated for 30 min with the following treatments: vehicle (saline); 1 μmol/L PKG I inhibitor DT3 (RQIKIWFQNRRMKWKKLRKKKKKH, Merck Millipore); 1 μmol/L sGC inhibitor ODQ (1H-[1,2,4]oxadiazolo[4,3,-a] quinoxalin-1-one, Sigma-Aldrich). The tissue was processed to determine RNA, protein or cGMP levels.

In Vitro Experiments

Murine inner medullary collecting duct cell line (mIMCD3, ATCC) or human mesangial cells (HMC) were obtained and cultured according to previously described procedures (23,36,37). To deplete ILK, semiconfluent cells were transfected with Metafectene (Biontex) and a combination of different small interference RNAs against ILK (si-ILK, Gene Link) or scrambled siRNA (Life Technologies), 20 nmol/L each. Once the convenient confluence was reached,

the cells were serum deprived for 24 h before the 30 min pretreatment with ODQ (1 μmol/L) followed by CIS treatment (30 μmol/L) for 30 min or 24 h, depending on the experiment. ILK gene silencing was monitored by immunoblot in the cell extracts and cell viability or contractility assays were performed.

To analyze the cell viability *in vitro*, mIMCD3 cells cultured in a 24-well plate were either pretreated with ODQ or not and then treated with CIS in serum-free medium for 24 h. After incubation, 50 μL of 5 mg/mL 3-(4,5-dimethylthiazol-2-yl)-2,5-diphenyl-tetrazolium bromide solution (MTT, Sigma-Aldrich) were added for 4 h. Conversion of MTT into purple formazan by metabolically active cells estimates the extent of cell viability. After the medium was removed, the formazan crystals produced were dissolved in 500 μL of DMSO and the optical density was measured at the Multimode Plate Reader (test wavelength 570 nm, reference wavelength 690 nm, PerkinElmer). Cell viability was defined as the relative absorbance of treated versus untreated cells and expressed as the percentage of the basal level.

Planar cell surface area (PCSA) changes and phosphorylation of myosin light chain (MLC) at serine 19 were analyzed in 30 min CIS-stimulated HMC, since both are considered contractile-related consequences of stimuli such as CIS (40). HMC were either pretreated with ODQ or not pretreated 30 min before the 30 min of CIS treatment. For determination of PCSA changes, HMC were grown at low density in 20-mm plates before they reached confluence (38,39) and the medium was replaced by buffer A (20 mmol/L Tris, 130 mmol/L NaCl, 5 mmol/L KCl, 10 mmol/L sodium acetate, 5 mmol/L glucose, pH 7.45, 2.5 mmol/L calcium) before the treatments. Photographs of the same cells were taken with an inverted phase contrast microscope (TMS-F Photomicroscope) at a 150× magnification at times 0 and 30 min after the contractile CIS treatment. PCSA was determined by computer-aided planimetric techniques in every cell with a sharp margin suitable for the analysis. The phosphorylation changes in MLC were determined by immunoblot densitometries ratios of p-MLC versus GAPDH as endogenous control.

cGMP Measurements

The renal tissues were homogenized with ice-cold, ethanol, centrifuged and the cGMP extracts in the supernatant were evaporated, acetylated and quantified using an enzyme immunoassay kit (Cayman Chemical).

Immunohistochemical Analysis

After euthanasia, kidneys were harvested, fixed in formaldehyde, dehydrated by an increasing, ethanol gradient and embedded in paraffin. Three-μm slices were deparaffinized, rehydrated and treated with 3% hydrogen peroxide for 20 min to block endogenous peroxidase activity. After blocking in horse serum for 30 min, sections were incubated sequentially with the ILK antibody (Santa Cruz Biotechnology) for 24 h, then the secondary antibody and, finally, with an avidin/biotin horseradish peroxidase macromolecular complex (Vectastain ABC kit, Vector Laboratories). The peroxidase-conjugated activity was developed with diaminobenzidine (Dako) and counterstained with hematoxylin (Sigma-Aldrich). The images were obtained with Eclipse 50i microscope (Nikon).

Histological Analysis

CIS-induced renal injury was analyzed 72 h after the single CIS dose. The harvested kidneys were fixed, dehydrated and embedded in paraffin. Afterwards, tissue slices (5 μm) were mounted on poly-L-lysine glass slides (Thermo Fisher Scientific), deparaffinized and rehydrated prior to being stained. Hematoxylin–eosin staining (Sigma-Aldrich) was performed using standard procedures and histological changes were evaluated semiquantitatively by a pathologist in a blinded manner. Pictures were obtained using Nikon Eclipse 50i microscope.

The following parameters were evaluated and scored in 8 to 10 high-power fields per section, using a scoring system based on the percentage of damaged tubules per field (1, <25%; 2, 25% to 50%; 3, 50% to 75%; and 4, >75%) tubular necrosis, tubular dilatation and intratubular cast formation. The total injury was assessed as the sum of all the individual percentages. The mean score of every parameter analyzed was represented and compared statistically (41,42).

Protein Extraction and Immunoblot

The kidney samples or cultured cells were homogenized in a lysis buffer (10 mmol/L Tris-HCl, pH 7.6, 1% Triton X-100, 1 mmol/L EDTA, 0.1% sodium deoxycholate, 500 nmol/L $NaVO_4$, 50 nmol/L NaF, 1 mmol/L PMSF and Complete from Roche) and spun off. The supernatant protein concentrations were determined by DC-Protein Assay (Bio-Rad) and equal amounts were separated in SDS-PAGE gels and transferred to 0.2-μm-PVDF membranes (PerkinElmer). After blocking with 5% nonfat dried milk, the membranes were incubated with antibodies against sGC-β1, α-SMA, actin, GAPDH (Sigma-Aldrich), phosphorylated vasodilator-stimulated phosphoprotein in Ser 239 (P-VASP) (Merck Millipore), PKG-Iα (Stressgen, Enzo Life Science Inc.), ILK (Cell Signaling Technology Inc.), phosphorylated Myosin Light Chain 2 (Serine 19), TGF-β and MCP-1 (Santa Cruz Biotechnology) in Tween Tris-buffered saline (20 mmol/L Tris-HCl, 0.9% NaCl, 0.05% Tween 20). After peroxidase-conjugated secondary antibody incubation (Sigma-Aldrich or Dako) the immunoblots were developed with ECL detection reagents (Pierce) and subsequent exposures into ImageQuant LAS 500 chemioluminiscent detection chamber (General Electric Healthcare). Densitometry was measured using ImageJ software (NIH).

Reverse Transcriptase–Quantitative Polymerase Chain Reaction (RT-qPCR)

Total RNA from each sample was extracted with TRIzol, transcribed to cDNA with a high capacity cDNA RT kit, and 10 ng cDNA were amplified by TaqMan qPCR gene expression assays for PKG-Iα, MCP-1, TGF-β and β-actin. RT-qPCR

analysis was performed in a 7500 qPCR thermocycler by using SYBR Green Master Mix (products and apparel from Life Technologies, Thermo Fisher Scientific Inc.) to quantify sGCβ1, PDE5 or β-actin as endogenous control mRNAs with tandem primers CTT ACC AGA AGC AGA TAG CAT CC and AGG TCG TCC AGG TTC ATC AC, CGG CCT ACC TGG CAT TCT and GCA AGG TCA AGT AAC ACC TGA TT or GAC GGC CAG GTC ATC ACT AT and CTT CTG CAT CCT GTC AGC AA, respectively.

To quantify non-excised ILK mRNA, RT-qPCR analysis was performed by using SYBR Green Master Mix with primers GGG CTC TTG TGA GCT TCT GT and GAG TGG TCC CCT TCC AGA AT designed to recognize the cDNA sequence between exons within the floxed area number 6 and 7 (25,27,36). The normalized gene expression method ($2^{-\Delta\Delta CT}$) for relative quantification of gene expression was used.

Statistics

The data shown are the means ± SEMs of a variable number of experiments detailed in the figure legends. Some data, particularly those concerning experiments performed under a paired design (Western blot and PCR experiments) are given as percentages of the basal or control values. Except in the morphological studies, and after testing the normality of the distributions (Kolmogorov–Smirnov test), data were compared using one-way (nonpaired) or nested (paired) analysis of variance (ANOVA), followed by a multiple comparison test. The morphological data were analyzed with the Kruskal–Wallis test, followed by multiple comparisons with the Bonferroni correction. *P* values less than 0.05 were considered statistically significant.

RESULTS

ILK Depletion Upregulates the sGC-cGMP-PKG Axis in the Renal Cortex

A previous study established the conditions for successful ILK depletion in the renal tissue of adult mice (24). Three weeks after tamoxifen (the ILK depletion inductor agent) or vehicle injection and before any experiment, the three-month-old mice were routinely genotyped by conventional PCR of the tail tip DNA. Those displaying successful depletion of ILK were used as cKD-ILK. Any direct effect of tamoxifen on sGC and PKG renal cortex content and glomerular filtration rate was excluded by treating the parental CRE and LOX mice with the drug (data not shown). To study whether ILK depletion was maintained during prolonged times, we determined by RT-qPCR the nonfloxed ILK levels in the renal cortex from vehicle-treated WT and TX-treated CRE-LOX mice at 1 month or 3 months after TX treatment (36), displaying similar ILK depletion levels at both ages (data not shown).

We evaluated the content and activity of the cGMP-related enzymes sGC and PKG in our animal model under basal conditions. Increased mRNA and protein levels of both sGC and PKG are present in cKD-ILK renal cortex when compared with WT animals (Figures 1A, B; 2A, B). After 24 h administration of the NO-donor isosorbide dinitrate (IDN), the expected reductions of sGC and PKG levels were observed in both groups of animals (9,21,43). These cGMP-related proteins content reductions, which are probably the main mechanisms of the pharmacological tolerance to NO, were less marked when ILK was depleted, since the sGC and PKG levels were significantly higher in NO-treated cKD-ILK than in NO-treated WT (Figures 1A, B; 2A, B).

We studied the cGMP levels produced by the increased sGC content in the renal cortex from ILK depleted animals. As anticipated, the basal level of cGMP

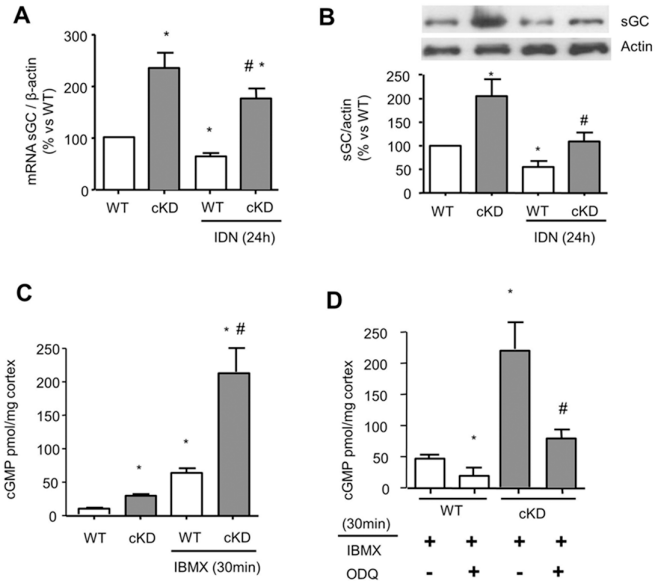

Figure 1. Renal ILK depletion increases soluble guanylate cyclase (sGC) expression and activity in basal conditions and after nitric oxide (NO) donor treatment. (A) sGCβ1 mRNA levels fold change in basal renal cortex determined by RT-qPCR, and normalized against β-actin as endogenous control. (B) Representative immunoblots and densitometric analysis of renal cortex sGCβ1 (70 KDa) normalized against actin, from WT and cKD mice in basal conditions or treated with 300 mg/kg body weight, orally NO-donor isosorbide dinitrate (IDN) for 24 h. (C) cGMP levels (pmol/ mg tissue) from basal WT and cKD renal cortex treated *ex vivo* with or without PDEs inhibitor IBMX (100 μmol/L) for 15 min. (D) cGMP levels from WT and cKD-ILK renal cortex pretreated *ex vivo* with IBMX 15 min and treated 30 min with the sGC inhibitor ODQ (1 μmol/L). All values are represented as mean ± SEM (% versus basal WT in A and B) $^{*}P < 0.05$ versus basal WT, $^{\#}P < 0.05$ versus treated WT. n = 10–15.

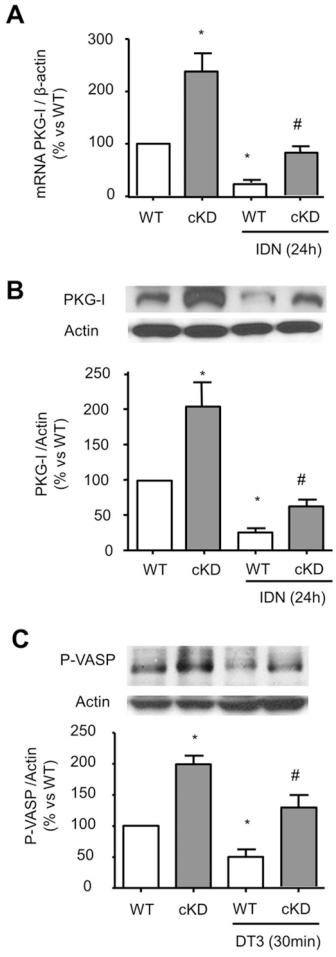

Figure 2. Renal ILK depletion increases cGMP-dependent protein kinase (PKG) expression and activity in basal conditions and after a nitric oxide (NO) donor treatment. (A) PKG-1α mRNA levels fold change in basal renal cortex determined by RT-qPCR and normalized against β-actin as endogenous control. (B) Representative immunoblots and densitometric analysis of renal cortex PKG-1α (76 KDa) normalized against actin from WT and cKD mice in basal conditions or after 24 h of treatment with the NO donor isosorbide dinitrate (NO) 300 mg/kg body weight, orally, for 24 h. (C) Representative immunoblots and densitometric analysis of renal cortex phosphorylated VASP in Ser 239 (P-VASP), 48 KDa normalized against actin from basal WT and cKD renal cortex treated *ex vivo* with PKG-1-α inhibitor DT-3 (1 μmol/L) for 30 min. All values are represented as mean ± SEM and % versus basal WT. $^{*}P < 0.05$ versus basal WT, $^{\#}P < 0.05$ versus treated WT, n = 10–15.

was increased in cKD-ILK, in accordance with the increased sGC content. More cortical tissue was incubated *ex vivo* with the wide-range PDE inhibitor IBMX for 30 min to avoid basal PDEs-dependent cGMP degradation (9,25). In this case, the differences between the groups were amplified (Figure 1C). Considering this IBMX-dependent cGMP-marked difference between the groups, we studied the specificity of the sGC-based cGMP production by cotreating more cortical tissue with IBMX and the sGC inhibitor ODQ for 30 min. As shown in Figure 1D, ODQ blunted the cGMP production in both animal groups (1D). Since the levels of PKG together with its activator cGMP were increased in the cKD-ILK renal cortex, we analyzed the PKG activity by determining the levels of phosphorylation of its substrate VASP at Ser 239 (4). cKD-ILK shows increased levels of basal VASP phosphorylation compared with WT (Figure 2C). We confirmed the specificity of the PKG-based VASP phosphorylation by using the pharmacological specific PKG-Iα Inhibitor DT-3 (1 μmol/L) for 30 min, which diminished VASP phosphorylation in both groups (44); however, PKG activity in the cKD-ILK tissue was significantly higher than in WT (Figure 2C).

ILK Depletion Increases Glomerular Filtration Rate after NO Donor Treatment

One month after the TX-induction, cKD-ILK and WT littermates were placed in metabolic cages to collect 24-h urine and glomerular filtration markers were determined. Basally, neither group of WT and cKD-ILK animals exhibited any comparative difference of plasma creatinine or clearance. However, the cKD-ILK treated for 24 h with the NO-donor IDN displayed significantly increased filtration when compared with the basal rates (Figure 3). No statistically significant differences in BUN or urinary albumin excretion were observed between the two basal groups (urinary albumin, mg per mg urinary creatinine, mean value ± SEM: WT 0.420 ± 0.06; cKD-ILK 0.504 ± 0.12;

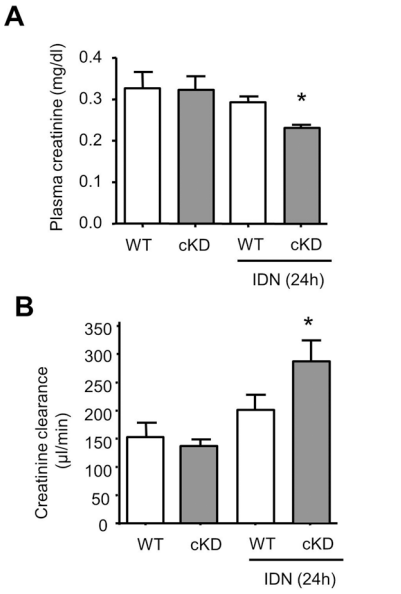

Figure 3. NO donor treatment increases glomerular filtration rate in cKD mice. (A) Plasma creatinine levels and (B) creatinine clearance were measured in WT and cKD mice under basal conditions or after 24 h treatment with 300 mg/kg body weight, orally of the NO donor isosorbide dinitrate (IDN) to evaluate glomerular filtration rate. The values are represented as mean ± SEM, $^{*}p < 0.05$ versus basal WT, n = 10–15.

BUN mg/dl plasma, mean value ± SEM: WT 24.23 ± 1.709; cKD-ILK 20.93 ± 2.139).

We reported no differences of basal filtration parameters between 1 month TX-induced or 3 months TX-induced animals. The plasma creatinine values (mg creatinine/dL plasma, mean value ± SEM) in animals 3 months after TX induction were WT 0.38 ± 0.026; cKD-ILK 0.41 ± 0.032. The BUN values (mg/dL plasma, mean values ± SEM) in animals 3 months after TX induction were WT 24.60 ± 3; cKD-ILK 26.2 ± 5.

CIS-Induced AKI Increases ILK Expression

Since there was no difference in time in the basal renal function of our ILK depletion model, we performed an experimental AKI model based on one single injection of CIS (10 mg/kg body weight) in 1-month TX-induced animals. Figure 4A shows that 3 d after

the single injection of CIS, the non-floxed ILK levels produced by the renal cortex determined by RT-qPCR were significantly increased in CIS-WT, while CIS-cKD-ILK mice showed the expected reduced levels as in the basal cKD-ILK animals (36). Figure 4B shows that ILK levels detected by immunohistochemistry in the renal tissue are reduced in both basal and CIS-treated cKD-ILK mice. The increase of ILK levels in CIS-WT mice by immunohistochemistry is difficult to assess, most likely due to dead cell debris present in the injured tissues (as scored in Figure 9).

ILK Depletion Maintains sGC-cGMP-PKG Axis Upregulation and Improves Glomerular Filtration under CIS-Induced AKI

To study the beneficial effect of ILK depletion under the CIS-based experimental AKI, we collected 24 h urine and plasma samples 3 d after the single injection of CIS in WT and cKD-ILK. All the CIS-treated animals showed increased plasma levels of creatinine and urea and decreased glomerular filtration rates. The depletion of ILK was protective, since lower creatinine and urea plasma levels and higher glomerular filtration rates were observed in the CIS-treated cKD-ILK group compared with the CIS-treated WT (Figure 5). TX itself did not contribute to the observed differences, as CRE and LOX mice treated with the drug exhibited the same degree of AKI as WT animals after CIS administration (data not shown).

The cortical sGC and PKG mRNA and protein expressions and their activity (measured as cGMP and VASP phosphorylation levels) were not affected by

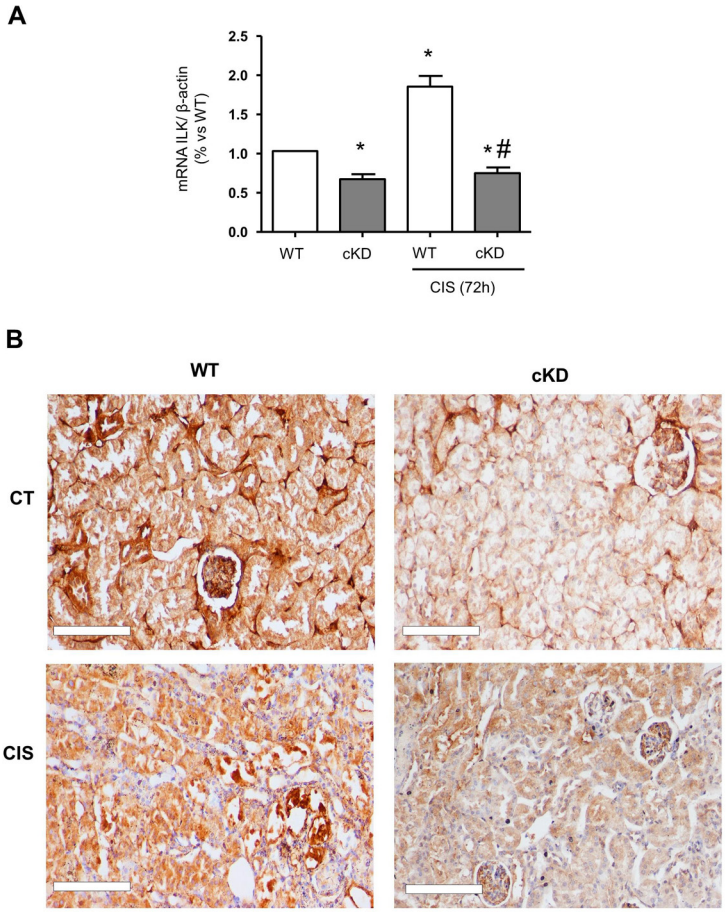

Figure 4. Renal ILK expression in CIS-induced AKI. (A) nonfloxed ILK mRNA levels fold change and normalized against β-actin as endogenous control determined by RT-qPCR in basal renal cortex from WT and cKD mice under basal or 72 h after a single injection of CIS (10 mg/kg body weight, IP). All values are represented as mean ± SEM and % versus basal WT. *P < 0.05 versus basal WT, #P < 0.05 versus treated WT, n = 10–15. (B) Representative microphotographs from ILK immunostained renal tissue sections of six different CIS-treated WT or CIS-treated cKD mice. Scale bar = 100 μm.

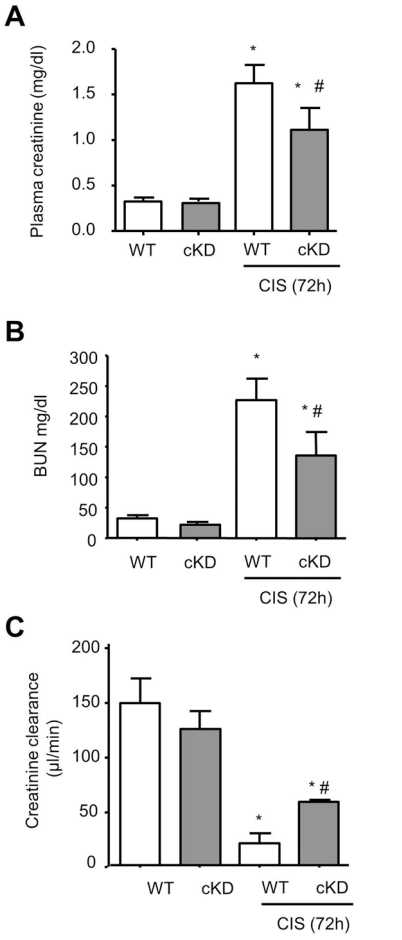

Figure 5. ILK depletion improves glomerular filtration rate in CIS-induced AKI. (A) Plasma creatinine, (B) blood urea nitrogen (BUN) and (C) creatinine clearance were measured in WT and cKD mice under basal conditions or 72 h after a single injection of CIS (10 mg/kg body weight, IP). The values are represented as mean ± SEM. *p < 0.05 versus basal WT, #P < 0.05 versus CIS WT, n = 10–15.

CIS itself, as compared with the basal conditions, but significant increased expression and activity was observed in CIS-treated cKD-ILK (Figure 6).

ILK Depletion Improves EMT and Inflammation Events in CIS-Induced AKI

CIS-based renal injury is associated with multiple mechanisms including tubular EMT and inflammation (1,2,3,4,5). Figure 7 panels A and B show that the renal cortex from CIS-treated WT has increased protein levels of the mesenchymal marker α-SMA together with the EMT inducer TGF-β. However, the increases were not observed in AKI-cKD-ILK mice.

The inflammatory mechanisms play an important role in the pathogenesis of CIS nephrotoxicity. We previously observed in cKD-ILK mice under a chronic renal insult by angiotensin II treatment that ILK depletion reduces proinflammatory markers such as MCP-1 (27). Figures 7C and D show increased cortical mRNA and protein levels of the inflammatory marker MCP-1 in CIS-induced AKI kidneys from both WT and cKD-ILK animals. However, the increased levels of MCP-1 were significantly lower in AKI-cKD-ILK when compared with AKI-WT. Hematoxylin–eosin staining in Figure 7E shows increased cellularity in the renal tissue of CIS-treated WT because of increased inflammatory cell recruitment and infiltration (1,2), which is less evident in CIS-treated cKD-ILK.

The Protective Effect of ILK Depletion on CIS-Induced AKI Depends on the sGC-cGMP-PKG Axis Upregulation: *In Vivo* and *In Vitro* Approaches

To emphasize that the upregulated cGMP axis may be one of the protective mechanisms followed by ILK depletion during CIS-induced AKI, we chose to pharmacologically modify the upregulated cGMP pathway during the CIS insult *in vivo* and *in vitro*.

First, we activated the cGMP pathway in the AKI-cKD-ILK mice by using a proper stimulus; since NO donors produce pharmacological tolerance that affects the amounts of sGC and PKG (Figures 1 and 2), we used 2.5 mg/kg body weight of a rather specific PDE5 inhibitor, Zaprinast (ZAP) (45,46) to increase the cGMP levels produced under ILK depletion and AKI conditions. As it has been demonstrated that PDE inhibitors alone (including ZAP) reduce the nephrotoxicity in AKI models (14,15,16,47,48), we used a suboptimal dose of ZAP, settled in 5–10 mg/kg body weight, (49,50).

As already shown in Figure 5, the parameters that measure glomerular filtration rate, creatinine and urea plasma concentrations and creatinine clearance were increased in the AKI animals, with less impairment in the CIS-treated cKD-ILK. ZAP positively enhanced the filtration in both WT and cKD-ILK CIS-treated animals. Interestingly, ZAP-treated cKD-ILK mice with CIS-induced AKI exhibit the maximum beneficial improvement of the ZAP administration, since creatinine, urea and creatinine clearance reached the basal conditions (Figures 8A, B). We observed no significant differences in cortical PDE5 mRNA levels between basal and CIS-induced AKI animals (Figure 8C).

We studied the protective role of cGMP upregulation in the tubular damage in CIS-treated animals. We studied the histological tubular damage and the protective role of ILK-dependent cGMP upregulation in CIS-treated WT with or without the ZAP cotreatment.

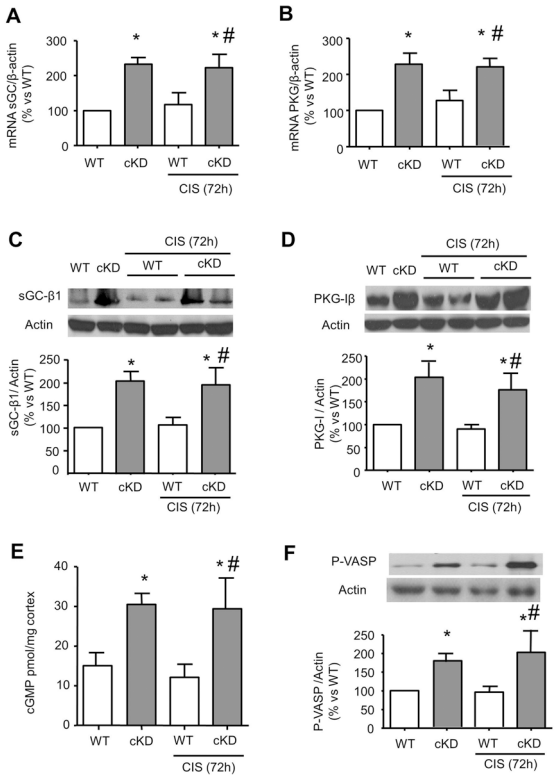

Figure 6. The ILK-dependent upregulation of soluble guanylate cyclase (sGC) and cGMP dependent protein kinase (PKG) remains in CIS-induced AKI. sGC and PKG expression and activity measurements in renal cortex from WT and cKD mice under basal conditions or 72 h after a single injection of CIS (10 mg/kg body weight, IP). (A) sGCβ1 and (B) PKG-1α mRNA levels fold change determined by RT-qPCR and normalized against β-actin as endogenous control. (C) sGCβ1 (70 KDa) and (D) PKG-1α (76 KDa) representative immunoblots and densitometric analysis normalized against actin. (E) cGMP levels (pmol/ mg tissue). (E) Phosphorylated VASP in 48 KDa Ser 239 (P-VASP) representative immunoblots and densitometric analysis normalized against actin. All values are represented as mean ± SEM (% versus basal WT in A–F). *$p < 0.05$ versus WT (basal), $^{\#}P < 0.05$ versus treated WT n = 10–15.

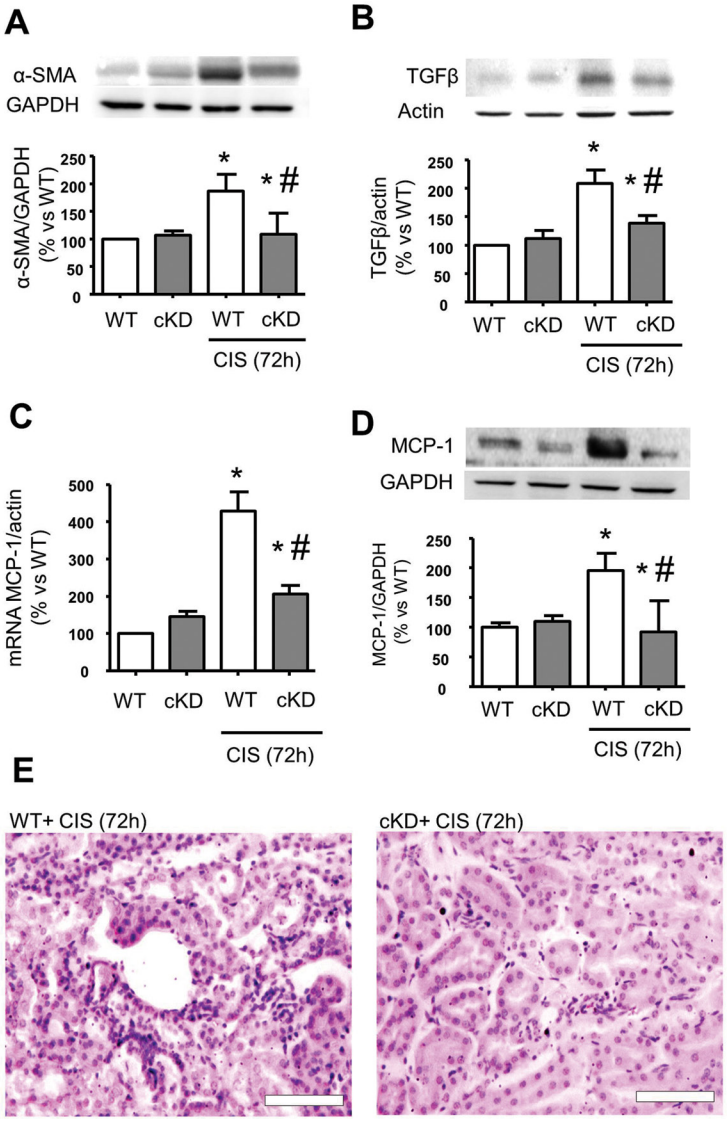

Figure 7. ILK-depletion improves EMT and inflammation events in CIS-induced AKI. All samples are from WT and cKD mice renal cortex under basal conditions or 72 h after a single injection of CIS (10 mg/kg body weight, IP). (A) α-SMA and (B) TGF-β representative immunoblots and densitometric analysis normalized against GAPDH or actin as endogenous control, respectively, and (B) TGF-β mRNA levels fold change determined by RT-qPCR and normalized against β-actin as endogenous control. (C) MCP-1 mRNA levels fold change determined by RT-qPCR and normalized against β-actin as endogenous control. (D) MCP-1 representative immunoblots and densitometric analysis normalized against GAPDH as endogenous control. The values are represented as mean ± SEM (% versus basal WT). *$p < 0.05$ versus basal WT, $^{\#}P < 0.05$ versus treated WT. n = 10–15. (E) Magnified interstitial areas from representative microphotographs from hematoxylin–eosin–stained renal tissue sections of six different mice. Scale bar = 100 μm.

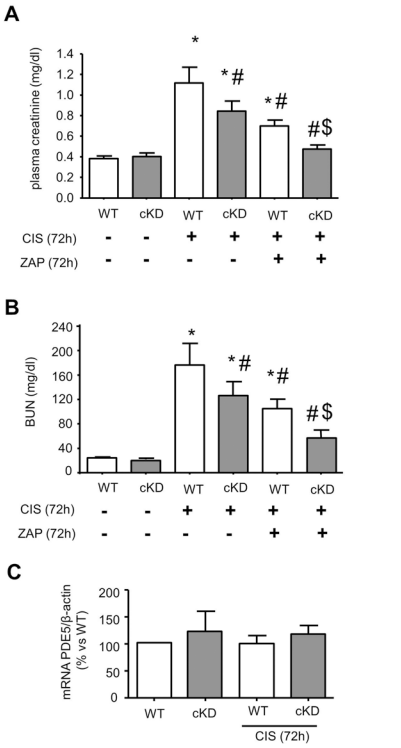

Figure 8. ILK-depletion together with pharmacological phosphodiesterase 5 (PDE5) inhibition enhances glomerular filtration rates in CIS-induced AKI. (A) Plasma creatinine and (B) blood urea nitrogen (BUN) levels were measured in WT and cKD mice under basal or 72 h after a single injection of CIS (10 mg/kg body weight, IP) together or not with a single suboptimal (2.5mg/kg body weight, IP) dose of the PDE5 inhibitor ZAP. (C) Additionally, PDE5 mRNA levels fold change in renal cortex determined by RT-qPCR and normalized against β-actin from WT and cKD mice under basal and AKI conditions were measured. The values are represented as mean ± SEM (% versus basal WT in C). *$p < 0.05$ versus basal WT, $^{\#}P < 0.05$ versus CIS WT, $^{\$}P < 0.05$ versus CIS cKD, n = 10–15.

After staining the kidney slices with hematoxylin–eosin, the histological tubular damage was studied for three traits: necrosis, intratubular protein cast and tubule dilation. Every injury was scored by the percentage of damaged tubules per total of the tubules present in the preparation. The total injury was assessed as the sum of all the individual percentages (41,42).

As shown in Figure 9, tubular damage was present in both groups, as a consequence of the CIS-dependent AKI. However, the depletion of ILK was protective, since the tubular injury scores showed a statistically significant decrease. ZAP improved the tubular damage in both AKI groups, but the maximum beneficial improvement was reached in the AKI-cKD-ILK group cotreated with ZAP,

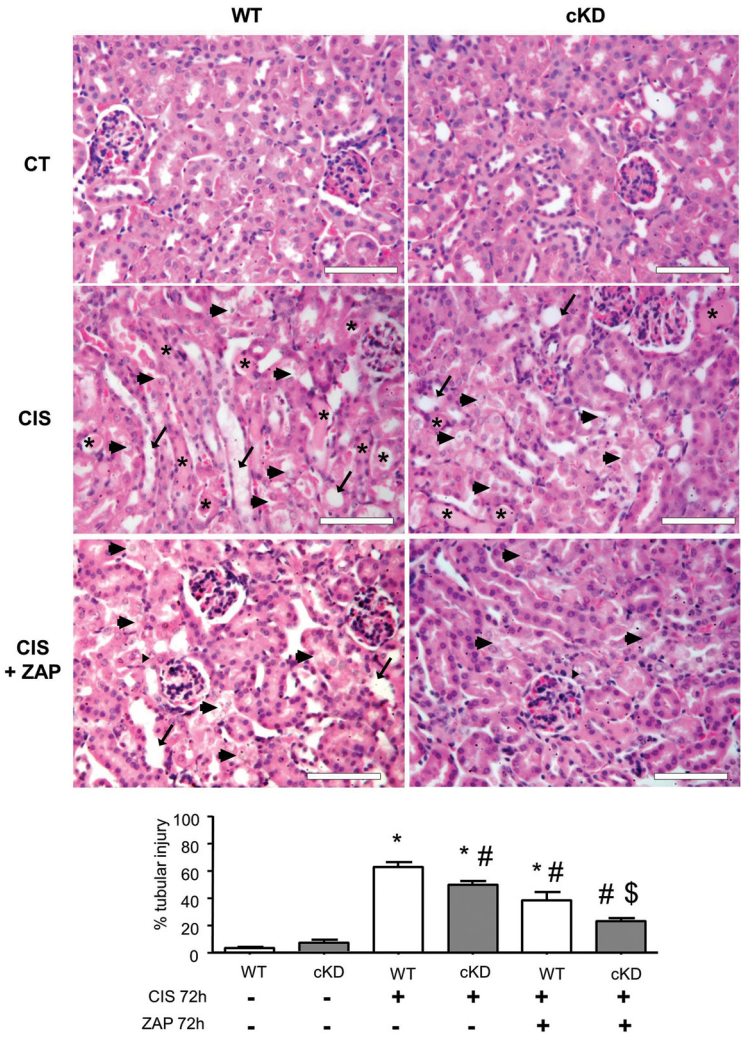

Figure 9. ILK depletion protects renal tubules in CIS-induced AKI and this improvement is enhanced by pharmacological phosphodiesterase 5 (PDE5) inhibition. Renal tissue sections from WT and cKD mice under basal or 72 h after a single injection of CIS (10 mg/kg body weight, IP) together or otherwise with a single dose (2.5 mg/kg body weight, IP) of PDE5 inhibitor ZAP, were stained with hematoxylin–eosin. Representative microphotographs from six mice, one from each group, and the representation of the semiquantitative assessment of tubular damage are shown (arrows show tubular dilatation, arrowheads show necrotic epithelial cells and stars show cast formation, scored as described in Materials and Methods. Scale bar = 100 μm. The values are represented as mean ± SEM of tubular damage score percentage. $^{*}p < 0.05$ versus basal WT, $^{\#}P < 0.05$ versus CIS WT, $^{\$}P < 0.05$ versus CIS cKD. n = 6.

where the tubular damage dropped to nonaffected basal levels.

To reinforce that ILK-dependent upregulation of cGMP axis may be one of the protective pathways taken by ILK depletion during CIS-dependent cytotoxicity, we cultured mesangial (HMC) and tubular kidney (mIMCD3) cells, depleted their ILK content with specific siRNAs and treated them with CIS. Since we confirmed that ODQ is an excellent sGC blocking agent in renal cultured tissues *ex vivo* (Figure 1), we used it to revert the cGMP-based ILK-dependent protective effect *in vitro*, by pretreating the ILK-depleted cells with the same ODQ concentration (1 μmol/L) prior to the CIS treatment.

We previously published that ILK depletion in cultured HMC by specific siRNAs significantly reduces the levels of ILK (28) and also that cGMP-related proteins are upregulated when ILK is modulated (23). Figure 10 confirms that ILK-depletion *in vitro* upregulates sGC and PKG in HMC (Figure 1A) and mIMCD3 (Figure 10D). A well-known toxic effect of CIS is to reduce the functional filtration in the glomeruli by increasing the contractility of the mesangial cells (1). It is already known that CIS is able to promote contractile-related events in cultured HMC (40). Thus, the CIS-based contractile capacity *in vitro* can be measured and quantified by the determination of the planar cell surface area (PCSA) reduction or the increased phosphorylation of the smooth muscle myosin light chain (MLC) at serine 19. We used these techniques previously in cultured HMC for this purpose (38,39). Figure 10B shows the PCSA reduction of HMC 30 min after CIS treatment (30 μmol/L). This event was compensated in ILK-depleted cells. ODQ pretreatment recovered the reduction of PCSA in the ILK-depleted HMC treated with CIS. ODQ alone induced no significant effect in PCSA ratio. Figure 10C shows increased levels of phosphorylated MLC after CIS treatment during 30 min. The ILK depletion compensated the increased phosphorylation. The pretreatment with ODQ prior to CIS recovered the phosphorylation levels in the ILK-depleted HMC. ODQ itself did not induce any significant toxic effect in HMC. Another cytotoxic effect of CIS is to induce tubular cell death *in vitro* (1,15,51). Figure 10E shows that CIS (24 h, 30 μmol/L) produces a significant increase in cultured mIMCD3 cell death as determined by MTT analysis of cell viability. ILK depletion in mIMCD3 successfully protects against cell death, but the toxicity was recovered by ODQ. ODQ itself did not produce any toxic effect in mIMCD3.

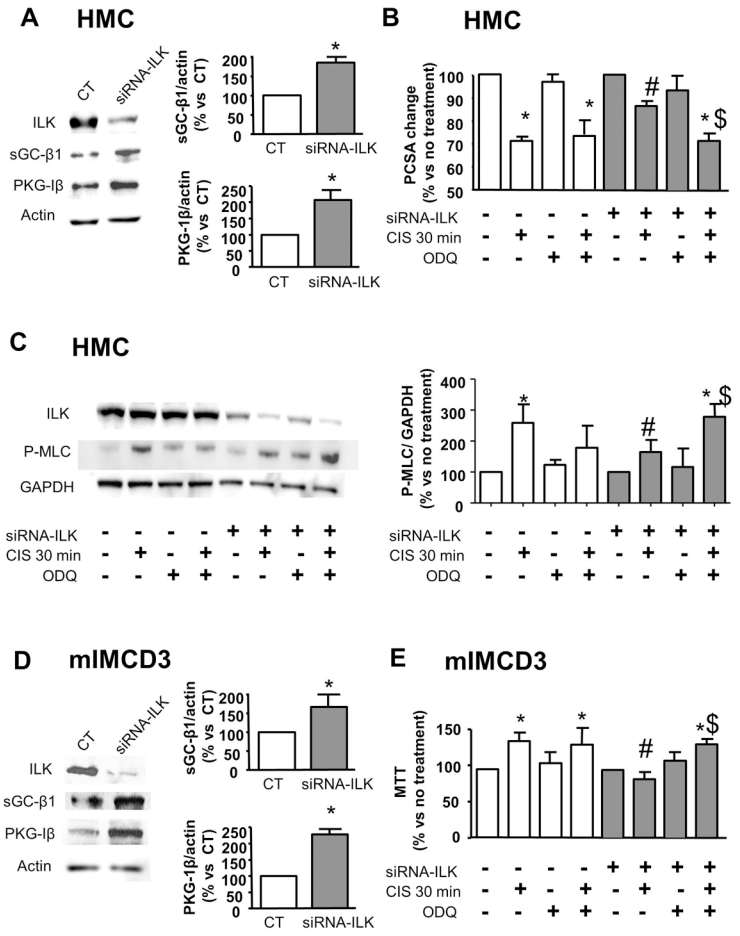

Figure 10. ILK depletion protects CIS-induced nephrotoxicity in cultured mesangial and tubular cells, while sGC blockade with ODQ restrained the protection. Cultured human mesangial cells (HMC) or tubular cell line mIMCD3 were transfected with specific siRNAs against ILK (siRNA-ILK) or scrambled siRNA as a transfection control. (A) Representative sGCβ1 and PKG-1α immunoblots and densitometric analysis normalized against actin as endogenous control in HMC protein extracts. ILK immunoblot shows the successful ILK depletion in HMC. (B) PCSA changes after CIS contractile treatment for 30 min with or without ODQ pretreatment for 30 min (1 μmol/L). (C) Representative phosphorylated myosin light chain in serine 19 (P-MLC) immunoblots and densitometry analysis normalized against GAPDH as endogenous control in HMC protein extracts. ILK immunoblot shows the successful ILK depletion. (D) Representative sGCβ1 and PKG-1α immunoblots and densitometry analysis normalized against actin as endogenous control in mIMCD3 protein extracts. Representative ILK immunoblot shows the successful ILK depletion in mIMCD3. (E) MTT cell death assays after CIS treatment for 24 h with or without ODQ pretreatment for 30 min (1 μmol/L). All values are represented as mean ± SEM (% versus no treatment), $^{*}P < 0.05$ versus control untreated cells, $^{\#}P < 0.05$ versus control cells treated with CIS, $^{\$}P < 0.05$ versus siRNA-ILK-cells treated with CIS. n = 6.

DISCUSSION

Our present work demonstrates that ILK depletion is a beneficial regulator of renal function, particularly when the kidneys are affected by CIS-based therapy. The ILK depletion upregulates the sGC-cGMP-PKG axis in the renal cortex, consistent with our previous approach in the systemic vasculature studies *in vivo* (25) where we observed a subsequent reduction of the vascular resistance when the system was activated. Furthermore, the ILK depletion upregulates the sGC-cGMP-PKG axis in cultured glomerular mesangial cells (23) and in tubular cells.

ILK and downstream effectors have been implicated in the pathogenesis of proteinuria and nephritic syndrome (32,33). For instance, the use of a podocyte-specific ILK-deleted mice model resulted in marked albuminuria, glomerulosclerosis and kidney failure, leading to animal death at very early ages (34,35). However, we used an adult TX-based inducible model of ILK depletion in all the kidney cells with no basal filtration problems. The renal function of our adult cKD-ILK mice remained basally healthy, because renal filtration markers were unaltered 1 to 3 months after TX induction. Furthermore, histological studies did not show any structural change compared with the WT. However, there is a basal sGC-cGMP-PKG axis upregulation in cKD-ILK cortical tissue. The lack of filtration differences between basal groups may be explained by a powerful negative feedback of the cGMP pathway since the activated PKG increases the cGMP hydrolysis capacity of PDE5 by phosphorylation (9). The contention of cGMP levels is clearly supported by the magnified differences in cGMP levels between WT and cKD-ILK when PDEs were blocked with IBMX *ex vivo* in the cortical tissues. On the other hand, the ability of renal structures to maintain a constant glomerular filtration rate is a well-known phenomenon, even when relevant changes appear in the glomerular perfusion pressure or in the synthesis of local mediators. The extraordinarily efficient capacity of glomeruli to maintain an unaltered filtration, together with the negative feedback mentioned above that is elicited by the PKG upregulation, may explain the balanced normal glomerular function observed in our basal cKD-ILK.

To be sure of the functional relevance of the sGC-cGMP-PKG upregulation when ILK was depleted, a single oral load of a NO donor was administered to the animals, and plasma creatinine concentration and creatinine clearance were measured after 24 h. Administration of

the drug to the WT seemed to increase glomerular filtration rates, but no statistical significances were reached, probably due to the same compensation mechanisms explained above. By contrast, cKD-ILK treated with the NO donor exhibited a significantly increased glomerular filtration rate. The pharmacological tolerance to NO donors previously described (9,21,43) explains the decreased sGC and PKG protein content after the acute load of the NO donor. However, these pharmacological disadvantages were partially abolished by the ILK-depletion, since sGC and PKG levels of NO-treated cKD-ILK remained higher in comparison to NO-treated WT, and similar to basal WT values.

After analyzing the filtration functionality both basally and after sGC activation, we tested the possible beneficial effect of ILK depletion on the CIS-induced AKI model. CIS-based renal injury involves variable degrees of vascular damage, apoptosis, death of renal tubular epithelial cells, EMT, increased oxidative stress, inflammation or hypoxia between others (1–5,41,42,52).

A higher glomerular filtration rate was observed in AKI-cKD-ILK. This may be due to the maintained sGC and PKG protein content and activity upregulation in cKD-ILK cortical tissue after CIS-induced AKI. Kim, *et al*. previously observed no differences in cortical sGC and cGMP levels in CIS-treated WT rodents, although they described an impaired sGC-dependent cGMP generation in the renal medulla (53).

When the kidneys are damaged with CIS, the cGMP synthesis elicited by ILK depletion increases the vasodilatation in various renal vascular beds, with subsequent increase of blood flow in both the glomerular structures and peritubular compartments. One primary consequence is an overall prevention of the CIS-based glomerular filtration rate decrease. On the other hand, ILK-dependent cGMP-axis upregulation protects renal structures from the toxic effect of the drug. In this context, the ILK-dependent renal perfusion increase may facilitate the oxygen delivery to the renal structures, which, in turn, may improve the hypoxia or even diminish the synthesis of free radical associated with cell oxygenation changes, with subsequent beneficial effects on renal apoptosis. It has been also described that cGMP may exert a direct cytoprotective effect on renal cells under nephrotoxic agents, in part due to an increase in the heme oxygenase-dependent formation of antioxidant metabolites or by decreasing renal caspase-3 activation (9–16).

We previously observed that ILK depletion reduces proinflammatory markers such as MCP-1 in cKD-ILK mice under chronic renal insult by angiotensin II (27). Our present results confirmed that ILK depletion also diminished the CIS-induced inflammatory response in the kidney, possibly by reduced leukocyte recruitment and adhesion mediators. CIS also produces tubular EMT, which requires the induction of TGF-β and downstream mediators, including ILK, and the increase of mesenchymal markers such as α-SMA. (1–5). These EMT markers were diminished in AKI-cKD-ILK compared with WT. EMT is an important mechanism in the pathogenesis of kidney fibrosis common to all forms of chronic kidney disease (4,5). Although TGF-β was upregulated in AKI-WT mice, the literature is consistent in demonstrating no significant ECM accumulation in AKI kidneys after a single short episode of CIS-treatment (1,2). Finally, our *in vitro* approaches also demonstrated that CIS-based mesangial and tubular toxicity (1,15,40,51) was diminished when ILK was depleted.

The lack of ILK may follow a direct pathway protecting the kidney, but we emphasized the importance of the cGMP-axis upregulation mechanism initiated by ILK depletion by using more *in vivo* and *in vitro* approaches. To ensure that ILK depletion is beneficial in this CIS-induced kidney dysfunction, it is necessary to pharmacologically activate the upregulated sGC-cGMP-PKG axis to observe an increase in the filtration rates. To select an activator, we discarded the administration of NO donors because their use is associated with tolerance (9,21), a situation already observed in our basal conditions. We therefore exacerbated the cGMP increase by using a PDE5 inhibitor. These products have been used as cGMP-axis improvers in many instances, because no pharmacological tolerance has been reported (9). Moreover, PDE5 inhibitors have been shown to be cytoprotective in CIS-induced nephrotoxicity *in vivo* and in cultured tubular cells by mechanisms that are not well elucidated (15,16). We chose a suboptimal dose of the PDE5 inhibitor ZAP (49,50) to avoid a veiling effect over the ILK-induced cGMP upregulation. Our histological and functional studies demonstrated that sGC-cGMP-PKG upregulation in ILK-depleted renal tissue improves renal functionality and somehow protects the tubular integrity under the CIS insult. These improvements were exacerbated by the use of the PDE5 inhibitor. Taken together, these strategies are finally translated into better filtration rates that almost reach the healthy animals' basal conditions.

Finally, sGC inhibitor ODQ was able to block the cGMP-based cytoprotective effect initiated by ILK depletion in two types of cultured renal cells under CIS-based cytotoxicity. ILK depletion protected against CIS-based contractility-related events in HMC and CIS-based cell death in tubular cells (1,39,40), but the protective effect was blocked by ODQ. These results give relevance to the ILK-based upregulation of cGMP axis as one of the potential cytoprotective mechanism observed in our settings.

CONCLUSION

The impairment in the glomerular and tubular function is a consequence of AKI, as the one present in the nephrotoxic effect of CIS treatment. A therapeutic approach to ameliorate AKI would be to increase the vasorelaxing and cytoprotective activity of cGMP. Unfortunately, the current available clinical treatments such as NO-based sGC activators have failed to be beneficial in

AKI management because sGC and PKG are quickly downregulated.

Here we demonstrated that renal depletion of ILK in an adult mice model and cultured mesangial and tubular cells upregulate the expression and functionality of the cGMP-axis–related sGC and PKG. The consequences are increased glomerular filtration rate and renal cytoprotective mechanisms under the CIS-induced AKI models. Our results suggest ILK as a novel therapeutic target that could ameliorate the renal impairment present in AKI.

ACKNOWLEDGMENTS

This work was supported by grants from the Spanish National Program for Research, Development and Innovation and cofunded by the Instituto de Salud Carlos III and FEDER funds (PI/11/01630, PI/14/01939, PI/14/02075 and FEDER funds ISCIII RETIC REDinREN programs RD06/0016/0002 and RD12/0021/0006) and the Spanish Ministerio de Ciencia e Innovación (SAF 2010-16198).
JL Cano-Peñalver was supported by a fellowship from the Spanish Ministerio de Ciencia e Innovación (BES 2011-045069).
We would like to thank S Dedhar for facilitating the floxed-ILK mice to establish cKD-ILK mice in our laboratory, and P Cannata for helping us during the setting of the histological analysis.

DISCLOSURE

The authors declare they have no competing interests as defined by *Molecular Medicine*, or other interests that might be perceived to influence the results and discussion reported in this paper.

REFERENCES

1. Sánchez-González PD, López-Hernández FJ, López-Novoa JM, Morales AI. (2011) An integrative view of the pathophysiological events leading to cisplatin nephrotoxicity. *Crit. Rev. Toxicol*. 41:803–821.
2. Carvalho Rodrigues MA, Martins NM, dos Santos AC. (2012) Cisplatin-induced nephrotoxicity and targets of nephroprotection: an update. *Arch. Toxicol*. 86:1233–1250.
3. Pabla N, Dong Z. (2008) Cisplatin nephrotoxicity: mechanisms and renoprotective strategies. *Kidney Int*. 73:994–1007.
4. Kim MK, *et al*. (2013) The differential expression of TGF-β1, ILK and wnt signaling inducing epithelial to mesenchymal transition in human renal fibrogenesis: an immunohistochemical study. *Int. J. Clin. Exp. Pathol*. 6:1747–58.
5. Burns WC, Thomas MC. (2010) The molecular mediators of type 2 epithelial to mesenchymal transition (EMT) and their role in renal pathophysiology. *Expert Rev. Mol. Med*. 12:e17.
6. Sanz AB, Sanchez-Niño MD, Martín-Cleary C, Ortiz A, Ramos AM. (2013) Progress in the development of animal models of acute kidney injury and its impact on drug discovery. *Expert Opin. Drug Discov*. 8:879–95.
7. Kaushal GP, Shah SV. (2014) Challenges and advances in the treatment of AKI. *J. Am. Soc. Nephrol*. 25:877–883.
8. Lieberthal W, Nigam SK. (2000) Acute renal failure. II. Experimental models of acute renal failure: imperfect but indispensable. *Am. J. Physiol. Renal Physiol*. 278:F1–12.
9. Francis SH, Busch JL, Corbin JD, Sibley D. (2010) cGMP-dependent protein kinases and cGMP phosphodiesterases in nitric oxide and cGMP action. *Pharmacol. Rev*. 62:525–563.
10. Agostino PV, Plano SA, Golombek DA. (2007) Sildenafil accelerates reentrainment of circadian rhythms after advancing light schedules. *Proc. Natl. Acad. Sci. U. S. A*. 104:9834–9.
11. Aversa A, *et al*. (2007) Chronic sildenafil in men with diabetes and erectile dysfunction. *Expert Opin. Drug Metab. Toxicol*. 3:451–64.
12. Prickaerts J, *et al*. (2002) Effects of two selective phosphodiesterase type 5 inhibitors, sildenafil and vardenafil, on object recognition memory and hippocampal cyclic GMP levels in the rat. *Neuroscience*. 113:351–61.
13. Polte T, Hemmerle A, Berndt G, Grosser N, Abate A, Schröder H. (2002). Atrial natriuretic peptide reduces cyclosporin toxicity in renal cells: role of cGMP and heme oxygenase-1. *Free Radic. Biol. Med*. 32:56–63.
14. Guan Z, Miller SB, Greenwald JE. (1995) Zaprinast accelerates recovery from established acute renal failure in the rat. *Kidney Int*. 47:1569–75.
15. Maimaitiyiming H, *et al*. (2013) Increasing cGMP-dependent protein kinase I activity attenuates cisplatin induced kidney injury through protection of mitochondria function. *Am. J. Physiol. Renal Physiol*. 305:F881–90.
16. Lee KW, *et al*. (2009) Sildenafil attenuates renal injury in an experimental model of rat cisplatin-induced nephrotoxicity. *Toxicology*. 257:137–43.
17. Lee YC, Martin E, Murad F. (2000) Human recombinant soluble guanylyl cyclase: expression, purification, and regulation. *Proc. Natl. Acad. Sci. U. S. A*. 97:10763–8.
18. Friebe A, Koesling D. (2003) Regulation of nitric oxide-sensitive guanylyl cyclase. *Circ. Res*. 93:96–105.
19. Lincoln TM, Dey N, Sellak H. (2001) cGMP-dependent protein kinase signaling mechanisms in smooth muscle: from the regulation of tone to gene expression. *J. Appl. Physiol*. 1:1421–30.
20. Omori K, Kotera J. (2007) Overview of PDEs and their regulation. *Circ. Res*. 100:309–27.
21. Filippov G, Bloch DB, Bloch KD. (1997) Nitric oxide decreases stability of mRNAs encoding soluble guanylate cyclise subunits in rat pulmonary artery smooth muscle cells. *J. Clin. Invest*. 100:942–8.
22. González-Santiago L, López-Ongil S, Rodríguez-Puyol M, Rodríguez-Puyol D. (2002) Decreased nitric oxide synthesis in human endothelial cells cultured on type I collagen. *Circ. Res*. 9:539–45.
23. De Frutos S, *et al*. (2005) Differential regulation of soluble guanylyl cyclase expression and signaling by collagens: involvement of integrin-linked kinase. *J. Am. Soc. Nephrol*. 16:2626–35.
24. Díez-Marqués ML, *et al*. (2006) Arg-Gly-Asp (RGD)-containing peptides increase soluble guanylate cyclase in contractile cells. *Cardiovasc. Res*. 69:359–69.
25. Serrano I, *et al*. (2013) ILK conditional deletion in adult animals increases cyclic GMP-dependent vasorelaxation. *Cardiovasc. Res*. 99:535–44.
26. McDonald PC, Fielding AB, Dedhar S. (2008) Integrin-linked kinase-essential roles in physiology and cancer biology. *J. Cell Sci*. 121:3121–32.
27. Alique M, *et al*. (2014) Integrin-linked kinase plays a key role in the regulation of angiotensin II-induced renal inflammation. *Clin Sci*. 127:19–31.
28. Gonzalez-Ramos M, *et al*. (2013) Integrin-linked kinase mediates the hydrogen peroxide-dependent transforming growth factor-β1 up-regulation. *Free Radic. Biol. Med*. 61:416–27.
29. Ortega-Velazquez R, *et al*. (2004) Collagen I up-regulates extracellular matrix gene expression and secretion of TGF-beta 1 by cultured human mesangial cells. *Am. J. Physiol. Cell Physiol*. 286:C1335–43.
30. Ortega-Velázquez R, *et al*. (2003) Arg-Gly-Asp-Ser (RGDS) peptide stimulates transforming growth factor beta1 transcription and secretion through integrin activation. *FASEB J*. 17:1529–31.
31. Li Y, *et al*. (2009) Inhibition of integrin-linked kinase attenuates renal interstitial fibrosis. *J. Am. Soc. Nephrol*. 20:1907–18.
32. Kretzler M, *et al*. (2001) Integrin-linked kinase as a candidate downstream effector in proteinuria. *FASEB J*. 15:1843–5.
33. Kang YS, *et al*. (2010) Inhibition of integrin-linked kinase blocks podocyte epithelial-mesenchymal transition and ameliorates proteinuria. *Kidney Int*. 78:363–73.
34. El-Aouni C, *et al*. (2006) Podocyte-specific deletion of integrin-linked kinase results in severe glomerular basement membrane alterations and progressive glomerulosclerosis. *J. Am. Soc. Nephrol*. 17:1334–44.
35. Dai C, *et al*. (2006) Essential role of integrin-linked kinase in podocyte biology: Bridging the integrin and slit diaphragm signaling. *J. Am. Soc. Nephrol*. 17:2164–75.
36. Cano-Peñalver JL, *et al*. (2014) Integrin-linked kinase regulates tubular aquaporin-2 content and intracellular location: a link between the extracellular matrix and water reabsorption. *FASEB J*. 28:3645–59.

37. Islas MS, *et al*. (2014) Antitumoral, antihypertensive, antimicrobial, and antioxidant effects of an octanuclear copper(II)-telmisartan complex with an hydrophobic nanometer hole. *Inorg. Chem*. 53:5724–37.
38 García G, *et al*. (2012) New losartan-hydrocaffeic acid hybrids as antihypertensive-antioxidant dual drugs: Ester, amide and amine linkers. *Eur. J. Med. Chem*. 50:90–101.
39. Iglesias-De La Cruz MC, Ruiz-Torres MP, De Lucio-Cazaña FJ, Rodríguez-Puyol M, Rodríguez-Puyol D. (2000) Phenotypic modifications of human mesangial cells by extracellular matrix: the importance of matrix in the contractile response to reactive oxygen species. *Exp. Nephrol*. 8:97–103.
40. Delbancut A, Lagroye I, Cambar J. (1994) Renal cytotoxicity of cisplatin in cultured glomerular mesangial and proximal and distal tubular cells. *Toxicol. In Vitro*. 8:517–9.
41. Jo SK, Cho WY, Sung SA, Kim HK, Won NH. (2005) MEK inhibitor, U0126, attenuates cisplatin-induced renal injury by decreasing inflammation and apoptosis. *Kidney Int*. 67:458–66.
42. Liu M, *et al*. (2006) A pathophysiologic role for T lymphocytes in murine acute cisplatin nephrotoxicity. *J. Am. Soc. Nephrol*. 17:765–74.
43. Dey NB, Busch JL, Francis SH, Corbin JD, Lincoln TM. (2009) Cyclic GMP specifically suppresses Type-Ialpha cGMP-dependent protein kinase expression by ubiquitination. *Cell Signal*. 21:859–66.
44. Dostmann WR, *et al*. (2002) Exploring the mechanisms of vascular smooth muscle tone with highly specific, membrane-permeable inhibitors of cyclic GMP-dependent protein kinase Ialpha. *Pharmacol. Ther*. 93:203–15.
45. Shah MK, Kadowitz PJ. (2002) Cyclic adenosine monophosphate-dependent vascular responses to purinergic agonists adenosine triphosphate and uridine triphosphate in the anesthetized mouse. *J. Cardiovasc. Pharmacol*. 39:142–9.
46. Tiboni GM, Lamonaca D. (2001) Transplacental exposure to methylene blue initiates teratogenesis in the mouse: preliminary evidence for a mechanistic implication of cyclic GMP pathway disruption. *Teratology* 64:213–20.
47. Dousa TP. (1999) Cyclic-3′,5′-nucleotide phosphodiesterase isozymes in cell biology and pathophysiology of the kidney. *Kidney Int*. 55:29–62.
48. Fernandes-Cerqueira C, *et al*. (2013) Concerted action of ANP and dopamine D1-receptor to regulate sodium homeostasis in nephrotic syndrome. *Biomed. Res. Int*. 2013:397391.
49. Irie K, *et al*. (2001) Inhibitory effects of cyclic AMP elevating agents on lipopolysaccharide (LPS)-induced microvascular permeability change in mouse skin. *Br. J. Pharmacol*. 133:237–242.
50. Sällström J, Jensen BL, Skøtt O, Gao X, Persson AE. (2010) Neuronal nitric oxide synthase supports Renin release during sodium restriction through inhibition of phosphodiesterase 3. *Am. J. Hypertens*. 23:1241–6
51. Sohn SJ, *et al*. (2013) In vitro evaluation of biomarkers for cisplatin-induced nephrotoxicity using HK-2 human kidney epithelial cells. *Toxicol. Lett*. 217:235–42.
52. Havasi A, Borkan SC. (2011) Apoptosis and acute kidney injury. *Kidney Int*. 80:29–40.
53. Kim CS, *et al*. (2012) Altered regulation of nitric oxide and natriuretic peptide system in cisplatin-induced nephropathy. *Regul. Pept*. 174:65–70.

Cite this article as: Cano-Peñalver JL, *et al*. (2015) Renal integrin-linked kinase depletion induces kidney cGMP-axis upregulation: consequences on basal and acutely damaged renal function. *Mol. Med*. 21:873–85.